Published in final edited form as:
Neuroimage. 2009 May 1; 45(4): 1173–1182. doi:10.1016/j.neuroimage.2008.12.071.

Multiexponential T_2 and Magnetization Transfer MRI of Demyelination and Remyelination in Murine Spinal Cord

Cheryl R McCreary[1,2,3], **Thorarin A Bjarnason**[4], **Viktor Skihar**[5], **J Ross Mitchell**[2,5], **V Wee Yong**[2,5], and **Jeff F Dunn**[1,2,3]

1*Experimental Imaging Centre, University of Calgary*

2*Hotchkiss Brain Institute, University of Calgary*

3*Department of Radiology, University of Calgary*

4*Department of Electrical and Computer Engineering, University of Calgary*

5*Clinical Neurosciences, University of Calgary*

Abstract

Identification of remyelination is important in the evaluation of potential treatments of demyelinating diseases such as multiple sclerosis. Local injection of lysolecithin into the brain or spinal cord provides a murine model of demyelination with spontaneous remyelination. The aim of this study was to determine if quantitative, multicomponent T2 (qT2) analysis and magnetization transfer ratio (MTR), both indicative of myelin content, could detect changes in myelination, particularly remyelination, of the cervical spinal cord in mice treated with lysolecithin. We found that the myelin water fraction and geometric mean T2 value of the intra/extracellular water significantly decreased at 14 days then returned to control levels by 28 days after injury, corresponding to clearance of myelin debris and remyelination which was shown by eriochrome cyanine and oil red O staining of histological sections. The MTR was significantly decreased 14 days after lysolecithin injection, and remained low over the time course studied. Evidence of demyelination shown by both qT2 and MTR lagged behind the histological evidence of demyelination. Myelin water fraction increased with remyelination, however MTR remain lower after 28 days. The difference between qT2 and MTR may identify early remyelination.

INTRODUCTION

Multiple Sclerosis (MS) is an autoimmune disease of the central nervous system that can affect both physical and cognitive functions. Brain and/or spinal cord lesions exhibit numerous processes including inflammation, edema, demyelination, remyelination, axonal loss, and gliosis (Lucchinetti et al., 2000, Markovic-Plese and McFarland, 2001). These lesions are often identified on conventional magnetic resonance imaging (MRI) examination; however, specificity of the pathophysiological origins of changes in proton density, T1, and T2 weighted MR signal intensities remains unclear (Pirko and Johnson, 2008).

Correspondence to: Cheryl McCreary, PhD, Heritage Medical Research Building, Rm 182B, 3330 Hospital Drive NW, Calgary, AB, T2N 4N1, Phone: (403) 210-9829, Email: E-mail: crmccrea@ucalgary.ca.

Studies have shown that magnetization transfer ratio (MTR) and short component T2 fraction, or myelin water fraction (MWF), are both related to myelin content. Although MWF and MTR are related, there is evidence that these methods are sensitive to different pathologies (Vavasour et al., 1998, Tozer et al., 2005). MTR may reflect myelin content as well as changes in inflammation (Blezer et al., 2007), edema (Gareau et al., 2000), and axonal density (Schmierer et al., 2004) while MWF may be more directly related to myelin content (Gareau et al., 2000, Davies et al., 2003). The primary goal of this study was to detect serial changes in multiexponential, quantitative T2 (qT2) and MTR during demyelination and remyelination caused by direct injection of lysolecithin into murine spinal cords.

In magnetization transfer imaging, selective off-resonance irradiation of the macromolecular proton pool reduces the observed mobile proton pool signal through magnetization transfer between these two proton pools (Wolff and Balaban, 1994, Henkelman et al., 2001). MTR compares the signal intensities in images with unsaturated and saturated macromolecular proton pools. Since myelin is the dominant source of macromolecular protons in white matter, MTR may be considered an indirect measure of myelin (Rademacher et al., 1999, Schmierer et al., 2007)

Spin-spin or transverse relaxation describes the loss of spin phase coherence, which depends on the local environment and diffusion. In tissue, the local environment is heterogeneous and results in multiple T2 relaxation rates. Although qT2 is not a direct measure of myelin, a number of studies have found that a short T2 component is associated with myelin content (Beaulieu et al., 1998, Webb et al., 2003, MacKay et al., 2006). This short T2 component between 10-50 ms is believed to originate from protons in water trapped between the phospholipids bilayers of the myelin sheath (MacKay et al., 2006). Nonaqueous protons in lipids and proteins have much shorter T2 values and direct signal from these components decay prior to detection.

Laule *et al*. showed that MWF was correlated with areas of demyelination and remyelination identified using histology in post mortem multiple sclerosis lesions (Laule et al., 2006). It has also been shown that MTR increases to control levels in lesions that have remyelinated (Deloire-Grassin et al., 2000, Chen et al., 2008). Merkler *et al*. (2005) found that a combination of T1, T2, and MTR gave the best discrimination of demyelinated, remyelinated, and normal white matter. Studies comparing single exponential T2 and MTR and studies comparing qT2 and MTR have been reported (Dousset et al., 1995, Vavasour et al., 1998, Gareau et al., 2000, Papanikolaou et al., 2002, Mottershead et al., 2003, Cook et al., 2004, Papanikolaou et al., 2004, Schmierer et al., 2004, Merkler et al., 2005, Odrobina et al., 2005, Tozer et al., 2005), however, *in vivo* time-course of changes in both qT2 and MTR have not been compared in model of demyelination and remyelination.

One model of focal demyelination with spontaneous remyelination involves direct injection of lysolecithin or lysophosphatidyl choline (LPC) into white matter tracks. A 1% LPC solution has been shown to solubilize myelin with little axonal damage in mouse spinal cord (Hall, 1972). White matter regions demyelinated by LPC injection remyelinate relatively quickly in the mouse (Jeffery and Blakemore, 1995). This model was chosen in part because the location of the lesion is known and can be easily located on MRI. In addition, the model involves changes in myelin with little edema and remyelination occurs within weeks, which makes tracking changes using MRI feasible.

In this study, we measured the time course of changes in MTR and qT2 in the lysolecithin murine model of demyelination with spontaneous remyelination. Cervical spinal cords of mice were injected with LPC and were imaged over 4 weeks following LPC injection. MTR and qT2 results were compared with histological evaluation of myelin. The objectives of this study were to determine 1) if *in vivo* MTR and qT2 could detect changes in myelin caused by LPC

injection into the mouse spinal cord, and 2) if the time course of changes in MTR and MWF were similar to histological markers of myelin.

METHODS

Murine Lysolecithin Model

Adult (6-8 week, 23-29 g) C57BL/6 male mice were obtained from Charles River (Montreal, Canada) and housed in groups of 2-4 under a 12/12 hour light/dark cycle with free access to food and water. All experimental procedures were performed in accordance with guidelines of the Canadian Council on Animal Care. Protocols were approved by the local experimental ethics committee.

Mice were anesthetized intraperitoneally with a mixture of ketamine (100 mg/ml) and xylozine (100 mg/ml). A 1 μl solution containing 1% D-lysophosphatidylcholine (lysolecithin; Sigma, St. Louis, MO) was injected over 1.5 min into the dorsal funiculi of the C5 spinal cord segment using a 32 G needle, attached to a 5 μl Hamilton syringe (Hamilton Company, Reno, USA). The needle was left in the spinal cord for an additional 2 minutes to prevent backflow of the lysolecithin. Muscles, connective tissue and skin were sutured above the injection site and the mice were allowed to recover.

MR imaging was performed 7, 14, 21, and 28 days post injection (dpi). Seven mice were imaged serially at the four time points. Three additional mice were imaged at each of the four time points studied for a total of 12 animals; these animals were sacrificed for histological evaluation after imaging. One 21 dpi sample was damaged during dissection and was not included in the histological analysis.

MR Imaging

During imaging, mice were anaesthetized with 2-2.5% isofluorane and were placed prone in a custom built holder in a 35 mm diameter birdcage coil. A pneumatic pillow was placed between the mouse chest and the holder. An MR compatible small animal monitoring and gating system (Model 1025, Small Animal Instruments Inc, Stonybrook, NY) was used to monitor respiratory rate and maintain body temperature of the anaesthetized mouse during imaging. Axial, sagittal, and coronal FLASH images were acquired for slice positioning. Intervertebral discs were used to locate the site of LPC between cervical vertebrae 5 and 6 (Figure 1).

Multi-echo spin echo (SE) images (TR/TE=3000/5 ms, inter-echo spacing = 5ms, 64 echoes, NA=4, FOV = 1.92×1.92 cm, matrix=128×128, slice thickness = 0.75mm, resolution=0.15mm) were acquired on a 9.4T Bruker Avance system. Single slice SE images with and without off-resonance pulses were also acquired for calculation of the magnetization transfer ratio (TR/TE=4000/15 ms with 40 pulses with an amplitude of 4μT, duration of 15ms, and interpulse delay of 1 ms were applied 2 kHz off-resonance, NA=2, FOV=2×2 cm, matrix=256×128, slice=0.75mm, resolution=78×156μm).

MR Data Analyses

The mean signal intensity from a region of interest (ROI) outlining the dorsal funiculus was used for T2 and MTR analyses. For T2 analysis, ROIs were drawn using third echo image which showed the best contrast between grey and white matter. The signal intensity decay curves from the multiecho images were fit with a regularized NNLS algorithm with the smoothing constraint $1.001\chi^2_{min} \leq \chi^2 \leq 1.0015\chi^2_{min}$ using AnalyzeNNLS (http://sourceforge.net/projects/analyzennls/). The T2 distributions were separated into 3 regions: myelin water fraction (MWF) 7.5-25ms, intra/extracellular water fraction (IEWF)

25-100ms, and long T2 fraction 100-640ms. Geometric mean T2 and the peak areas were determined for each region (Whittall et al., 1997).

The signal to noise ratio (SNR) was calculated for each experiment as the mean signal intensity of the dorsal column on the first echo image divided by the standard deviation of a region of interest drawn in air.

For MTR analysis, ROIs were drawn using the spin echo image with saturation pulses for better contrast between grey and white matter. Although the ROIs for qT2 and MTR analyses were drawn separately because of slightly different in-plane resolutions between the data sets, they encompassed the entire dorsal funiculus. MTR was calculated as the difference between average signal intensity from the dorsal funiculus ROI with and without saturation pulses, normalized to the signal intensity without saturation pulses and is expressed in percentage units.

Histological Preparation and Staining

Mice were deeply anaesthetized and perfused transcardially with PBS followed by 4% paraformaldehyde solution (in PBS). Spinal cords were exposed, dissected out and immersed in 4% paraformaldehyde solution for overnight fixation followed by 30% sucrose for 3 days. The C2 and T1 spinal cord segments were separated as one block using a scalpel blade. Ten μm frozen sections were cut on the Leica Cryostat (Leica Instruments GmbH, Nusslock, Germany), immediately mounted onto slides and stored at −20°C.

Eriochrome Cyanine Staining

Eriochrome cyanine with neutral red counter staining for myelin has been described previously (Kiernan, 1984). Briefly, ten micron thick cryosections of the spinal cord were air dried for at least 30 min and rehydrated in the series of descending ethanol concentrations (100, 95, 90, 79, and 50%). Sections were incubated for 15 min in the mixture of 0.2% of $FeCl_3$ and 0.080% of eriochrome cyanine (EC) in aqueous H_2SO_4. Sections were washed in distilled water, differentiated in 0.5% aqueous NH_4OH solution for 10 s, and counterstained with 1% neutral red solution for 1 min. Finally, sections were washed again in distilled water and dehydrated in a series of ascending ethanol concentrations.

The area of myelinated white matter in the dorsal column was determined using thresholding analysis available in ImageJ software (Rasband, 1997-2007) and expressed relative to the area of the dorsal column (Figure 2). 32-bit RGB tiff images were split in into three 8-bit grayscale images containing the red, green and blue components of the original. The dorsal column was outlined and an intensity threshold was applied to the red channel grayscale image. Relative areas from 3 to 5 sections for each sample were averaged. Sections were selected within 300 μm of the site of injection (*ie*. included in the MR slice), which was identified on the sections by the disruption of the dorsal surface, presence of a needle track, and lack of EC stain. The red channel was selected because it showed the greatest contrast between GM and WM.

Statistics

One way analysis of variance with Student-Newman-Keuls pairwise post-hoc testing was used to compare experimental groups where $p < 0.05$ was considered significant.

RESULTS

The geometric mean T2 values, relative area of each T2 component, and magnetization transfer ratios for the signal from the dorsal column were calculated for 4 healthy animals. qT2 and MTR values from the dorsal column of saline-injected mice were not significantly different

from values obtained from ROIs drawn in the white matter of the lateral spinal cord in treated animals. Examination of eriochrome-stained sections of lysolecithin-treated spinal cords showed that the myelin of the lateral white matter was intact and appeared normal. Therefore, qT2 and MTR values from the dorsal column of control mice and lateral white matter from treated mice were pooled together. The pooled data results in a control ROI for each of the 32 animals studied.

Quantitative T2 (qT2)

Example of the spin echo images from a single mouse are shown in Figure 3A-G. The ROI, drawn in red on the magnified image at the 25ms echo time (Figure 3H), outlines the dorsal column and the pixels that were used for analyses. The signal decay curve from this ROI and the residuals of the fit are shown in Figure 4A and B, respectively. The regularized NNLS fit results for all the time points studied in the same mouse are shown in Figure 4C-F. Two water compartments were found consistently, with an additional small long T2 component occasionally appearing which was observed at 21 dpi in this example. The long component (>100ms) was found in a portion of each of the experimental groups: 13 of 33, 6 of 10, 8 of 10, 8 of 10, and 4 of 10 mice in the control, 7, 14, 21, and 28 dpi groups, respectively. The SNR for the qT2 data ranged between 100 and 152 with a mean SNR (± SEM) of 133 ± 3.

The MWF was significantly decreased at 14 and 21 days post injection (dpi) and recovered to control values by 28 dpi (Figure 5A). In addition to the MWF changes detected, we found a shift in the geometric mean T2 of the intra/extracellular water component to significantly lower values at 14 and 21 dpi returning to control levels by 28 dpi (Table 1, Figure 6). No significant changes in the MWF or long T2 values were detected, although the variance in the long component fraction nearly doubled in the 14dpi group.

Magnetization Transfer Ratio

MTR values significantly decreased by approximately 10 percentage units (pu) at 14 dpi and remained low for the duration of the study (Table 1, Figure 5B).

Histology

Regions of demyelination were seen by the absence of blue EC staining sections of the spinal cord (Figure 7). In these sections, the neutral red counterstain showed the presence of numerous cells within the area of the lesion at 7 dpi. The density of infiltrating cells in the lesion decreased over time. The area of the lesion relative to the area of the dorsal column (mean ± SEM) was 45±5, 50±2, 21±10, and 21±10 % at 7, 14, 21, and 28 dpi respectively.

Oil red O lipid staining qualitatively showed a large number of dark red droplets within the area of the lesion at 7 dpi. The density of droplets within the lesion area decreased, but did not disappear entirely, over the time course examined.

DISCUSSION

The primary goal of this study was to compare serial changes in qT2 and MTR during demyelination and remyelination caused by direct injection of lysolecithin into murine spinal cords. Changes in myelin content of the dorsal column were successfully detected *in vivo* using multicomponent T2 and magnetization transfer imaging. Although neither MWF nor MTR followed the same time-course of myelination as observed by histology, we detected a difference in the time courses followed by the myelin sensitive MR measures. Changes in MWF paralleled eriochrome cycanine evaluation of myelin content but appeared to occur 1 week after histological changes. MTR results also decreased 1 week following the histological changes, however, MTR remained low throughout the duration of the study. The time course

of MWF followed histological evaluation of myelin changes more closely than MTR. Our results are consistent with a number of previous studies that have found both MTR and MWF are independent measures of myelin content (Vavasour et al., 1998, Gareau et al., 2000, Odrobina et al., 2005, Tozer et al., 2005)

Histology

Although we did not perform electron microscopy for definitive assessment of the remyelination in this study, the time course observed using EC evaluation of the lesion size is consistent with previous reports of demyelination and remyelination of lysolecithin lesions in murine spinal cord (Hall, 1972, Jeffery and Blakemore, 1995, Pavelko et al., 1998). Prominent demyelination was found by 7 dpi (Hall, 1972, Jeffery and Blakemore, 1995, Pavelko et al., 1998) and early evidence of remyelination was present 2 and 3 weeks after injection (Jeffery and Blakemore, 1995, Pavelko et al., 1998). The thickness of the myelin sheath and the number of remyelinated axons increasing significantly over the 13 dpi values by 5 weeks (Pavelko et al., 1998). Futhermore, numerous macrophages were found to infiltrate the lesion with little extracellular myelin debris at 7 dpi, with the number of infiltrating macrophages decreasing over time (Jeffery and Blakemore, 1995).

Hydrophobic esters of cholesterol are the principal lipids of degraded myelin, whereas hydrophilic phospholipids are predominant in normal myelin sheaths (Kiernan, 1990). This change in lipid content during degeneration of myelin allows histological differentiation of the two states. Eriochrome cyanine, a mordant-dye, stains phospholipids, while Oil red O is a lipid soluble dye capable of staining intracellular lipid droplets (Kiernan, 1990). We observed dark Oil Red O staining within the area of the lesion, which showed numerous infiltrating macrophages in EC-stained sections, suggesting that myelin debris was present within the infiltrating macrophages.

Quantitative T2

We found that MWF more closely reflected the time course of histological evaluation of myelin content than MTR, although detection of demyelination using MWF was delayed in comparison to eriochrome cyanine staining for myelin. It has been shown previously that MWF did not distinguish intact myelin from degraded myelin in rat sciatic nerve (Webb et al., 2003). The delay in MWF changes in response to demyelination observed in this study is most likely due to the presence of degraded myelin remaining in the lesion, which is supported by the large amount of Oil Red O staining for lipids at 7 dpi.

In addition to the changes in MWF, we found the geometric mean T2 of the intra/extracellular water (IEW) component decreased at 14 and 21 dpi compared to control and remained low at 28 dpi compared to 7 dpi measures. One possible explanation for this decrease in IEW geometric mean T2 may be an increase in the diffusion distance of water caused by the breakdown of myelin. Biton and co-workers found an increase in mean displacement of water using diffusion tensor imaging of myelin deficient rat spinal cord (Biton et al., 2006). Furthermore, Sun *et al*. found an increase in radial diffusivity in the demyelinated corpus collosum of mice treated with cuprizone (Sun et al., 2006). With the breakdown of barriers to diffusion, the exchange of magnetization between the IE water pool and myelin water would increase. In a 4-pool, or 2-pool, model of white matter, increasing the magnetization exchange rate between IE and myelin water shifted the IE water geometric mean T2 to shorter values (Stanisz et al., 1999, Bjarnason et al., 2005).

Another possible explanation for the observed decrease in the geometric mean T2 value of the intracellular/extracellular water component is related to the number of infiltrating macrophages

present within the lesion, which could increase the amount of non-myelin macromolecules and decrease T2 values. These speculative explanations require further investigation.

The pattern of change in T2 distribution observed in this study is contrary to those predicted by a model of demyelination, inflammation, and axonal loss in peripheral nerve (Odrobina et al., 2005). Odrobina et al suggested that in pure demyelination, the MWF would decrease; the IEWF would increase correspondingly, without any changes in the mean T2 values of each component. If demyelination and axonal loss were present, then MWF would decrease, IEWF would be unchanged but the T2 value of the IEW would increase. In a model of pure inflammation, Odrobina et al predicted that there would be an increase in the T2 value of the IEW. We found in our model of LPC-induced demyelination in the spinal cord that the MWF decreased with a corresponding increase in IEWF, however, the mean IEW T2 value decreased. In the tellurium model, demyelination is a result of an alteration in enzyme activity in myelinating Schwann cells which blocks cholesterol synthesis and down regulates major structural proteins in the peripheral nervous system (Harry et al., 1989). In contrast, the myelin sheath is selectively solubilized by into discrete lipoprotein units by the detergent action of LPC, initially maintaining the biochemical constituents of myelin until the debris is taken up by activated macrophages (Gent et al., 1964, Tipperman et al., 1984). Differences in the biochemical constituents between the tellurium- and LPC-induced demyelination could account for the different IEW T2 results in our study compared to Odrobina et al (Odrobina et al., 2005). Furthermore, a change in myelin structure could affect the exchange mechanisms between myelin water and IE water. If the demyelination process also increases the rate of exchange between theses two water compartments, which could be expected with structural breakdown of myelin, the measured position of the IE peak would be expected to decrease (Stanisz et al., 1999, Bjarnason et al., 2005). It is important to note that this LPC model of demyelination and remyelination involves some inflammation, but lacks significant edema which may be present in MS lesions. Further studies are required to examine these relationships with varying degrees of demyelination, inflammation, axonal loss, and gliosis.

We found either 2 or 3 T2 components in the mouse spinal cord, with the frequency of detecting a third component changing with lesion evolution. This long component falls in the range considered intracellular/extracellular water by Mackay et al (MacKay et al., 2006). This longer component appeared as a clearly separate peak in our data, which would be characterized better with data acquisition to longer echo times of 750 ms rather than 320 ms. Other *in vitro* studies have found 3 T2 components in spinal cord white matter (Stewart et al., 1993), rat and garfish optic nerve (Beaulieu et al., 1998, Bonilla and Snyder, 2007) and peripheral nerve (Does and Snyder, 1996, Webb et al., 2003, Stanisz et al., 2004, Odrobina et al., 2005), supporting the existence of more than 2 detectable water components. The long component found in our study is of relatively low intensity in comparison to previous reports and might be caused by spurious fitting of noise or motion artifacts; however, this is unlikely because we fit a DC offset to take into account the use of magnitude images and Rician distribution of the noise. Furthermore, the detection of a long component was not randomly distributed throughout the time course studied. It has been hypothesized that this long component, in the range of 200-800 ms, originates from extracellular water and may be important in the characterization of white matter pathologies like MS lesions or phenylketonuria (Laule et al., 2007a, Laule et al., 2007b).

The T2 distributions we measured are consistent with qT2 results reported for excised rat spinal cord at 7T. They found a MWF of 0.35±0.04 in the dorsal column with mean T2 of 11.5±1.2ms and 42.7±1.4 ms for the intermediate component (Kozlowski et al., 2008). MWF in bovine and human spinal cords have been reported and are similar to the values we report (Wu et al., 2006, Minty et al., 2009 in press)

Gareau et al and Graham et al have suggested a minimum signal to noise ratio of 270 and 500, respectively, is required for accurate and reliable determination of multiple T2 components (Graham et al., 1996, Gareau et al., 1999). Despite SNR values between 100 and 152, we detected a short T2 component in all multi-voxel ROIs with estimates of the MWF and T2 values with less than 10% standard error. Unlike Gareau et al (1999), we were able to detect a short T2 component in all mice despite a mean SNR of 132. The greater number of echoes (64 vs 32) with shorter the interecho spacing (5 vs 20 ms) used in our study decreased the SNR requirement for detection of multiple T2 components (Anastasiou and Hall, 2004).

Magnetization Transfer

A decrease in MTR was detected with demyelination, however, the MTR values did not return to control values with early remyelination. A number of previous studies found that MTR was strongly associated with myelin content, including detection of remyelination (Deloire-Grassin et al., 2000, Barkhof et al., 2003, Mottershead et al., 2003, Schmierer et al., 2004, Merkler et al., 2005, Chen et al., 2008) and that MTR returns to near control values with remyelination (Dousset et al., 1995, Chen et al., 2008). Repair of demyelination was indicated via the increase in the area of eriochrome cyanine stained tissue within the dorsal column over the 28 day duration of our current study. However, increases in myelin content were not reflected in the MTR values, in contrast to previous reports. Deloire-Grassin and colleagues found MTR values returned toward control levels 30 – 40 days after lysolecithin injection into the corpus callosum in rats (Deloire-Grassin et al., 2000). Although the 28 dpi time point in our study is similar to the 30 day in the work reported by Deloire-Grassin and colleagues, we found that MTR remained lower than control values. Perhaps this difference is related to differences in study design and analysis of the MTR data. We compared MTR values between a control group and 4 times after injection of lysolecithin. Deloire-Grassin used the MTR value from the side contralateral to the site of injection into corpus callosum as a reference and expressed changes in MTR as a percentage decrease from the reference, normal appearing white matter MTR. Although this approach uses an internal reference reducing variability within a study, it is not always possible to identify normal tissue to use as a reference.

In a different model of demyelination with spontaneous remyelination, Merkler et al found that the MTR of murine corpus callosum returned to control levels 12 weeks after withdrawal from a cuprizone diet, corresponding with the time course of remyelination (Merkler et al., 2005). Furthermore, both quantitative magnetization transfer imaging and MTR have been used to demonstrate differences between demyelinated and remyelinated MS lesions in post mortem human brain (Schmierer et al., 2004, Schmierer et al., 2007). These post mortem studies by Schmierer et al. found that MTR correlated with myelin content and that the MTR of remyelinated lesions was significantly different from both normal appearing white matter and demyelinated lesions. It is possible that an increase in MTR toward control values may have become evident if our study was lengthened. In planning this study, the duration of 4 weeks was based on previous studies which characterized the time course remyelination of LPC-treated the mouse spinal cord using histological techniques and showed rapid remyelination within 3 weeks (Jeffery and Blakemore, 1995, Pavelko et al., 1998, Larsen et al., 2003). Although histologically observable myelin was present within previously demyelinated areas at 4 weeks, more time may be needed for compaction and biochemical composition to develop, which could change magnetization transfer (Alberghina et al., 1983, Kucharczyk et al., 1994). Additionally, Schmeirer et al (2007) noted that MTR values in normal appearing white matter were slightly higher in post mortem samples compared to *in vivo* values. Differences between our animal model and the more complex pathologies present in MS lesions may contribute to the differences between our study and previous reports showing correlation between MTR and myelin content.

MTR is a semi-quantitative measure that depends on not only the size of the macromolecular pool but also the exchange rate between the bound and mobile proton pools. It is a complex function of many processes involving spin-lattice (T1) and cross-relaxation (Ropele et al., 2000). Quantitative MT may provide a more direct indication of myelin content, arguably making it a better choice for these experiments (Davies et al., 2003, Schmierer et al., 2007). However, we chose MTR rather than quantitative MT for this study because shorter imaging times are needed, data analysis is simpler, and fewer assumptions are made. Quantitative MT experiments measuring the size of the bound proton pool make assumptions regarding the number of proton pools in the sample and are relatively time consuming because they require multiple MT measurements as well as an independent measurement of T1 (Levesque et al., 2005). Most quantitative MT experiments assume that there is exchange between 2 proton pools: bound and mobile protons. However, more complex models may be needed; four pool models of exchange have been proposed (Stanisz et al., 1999, Sled and Pike, 2001, Bjarnason et al., 2005). Due to imaging time constraints, we did not measure T1 in this experiment so we are unable to determine whether this lower MTR is related to a change in direct saturation as a consequence in longer T1 values or is a consequence of MT changes.

It is possible that the MT acquisition parameters used in this study may not have been optimal for detecting changes in the short T2 component. A 4 pool model of magnetization exchange has been suggested, with each component having different T2 values and magnetization transfer effects (Vavasour et al., 2000, Bjarnason et al., 2005). The offset frequency, pulse amplitude, and number may be more sensitive to changes in the non-myelin solid pool rather than the myelin pool, but this is unlikely. We choose the number, amplitude and offset frequency of MT pulses based on providing the best contrast between grey matter and white matter.

Time course of changes in myelin markers: qT2, MTR, and histology

Neither MWF nor MTR detected the presence of early demyelination, which was evident on histological examination at 7 dpi. As discussed previously, the lack of detection by MR is likely due to the presence of myelin debris within macrophages present in the lesion (Jeffery and Blakemore, 1995, Webb et al., 2003). Furthermore, a freeze fracture study on macrophages from LPC-induced lesions in rat spinal cord showed that phagocytosed myelin initially retained its lamellar structure within vacuoles before eventual lysosomal digestion forms lipid filled vacuoles (Tipperman et al., 1984). This retained lamellar structure within macrophages may explain why MWF and MTR did not change from control levels when cross relaxation and exchange mechanisms depend on the restricted water environment created by the structure of intact myelin. Unfortunately, the time line for these changes was not reported but could be within 7 dpi.

Furthermore, in comparing histological results to MR measures it is important to consider the differences in the volumes sampled. A much smaller volume of tissue is sampled for histological sections when compared to MR. In this study, cryosections within 300 microns of the centre of the lesion were examined allowing for portions of incomplete remyelination to be visible. However MR techniques sample much larger volumes of tissue. Even with a sub millimeter slice thickness, partial volume effects are present which can make detection of small regions of demyelination and remyelination difficult. The ROI based analysis used in this study also contributes to partial volume effects. Partial volume effects could explain why MWF return to control levels while histological evidence of incomplete remyelination was present at 28 dpi.

Surprisingly, MTR values did not increase toward control levels after 28 days. One possible explanation for the difference between the MWF and MTR results at 28 dpi is that although myelin layers are formed, the lipid and/or protein content of the newly repaired myelin is

biochemically different from mature, compact myelin affecting magnetization transfer ratio. Protein content and lipid composition have been shown to change significantly during development in regenerating peripheral nerve (Alberghina et al., 1983) and the proportion of constituent lipids in myelin has been shown to alter MT effects (Kucharczyk et al., 1994). The protons saturated in an MTR experiment typically have T2 values in the range of 10 μs and are in exchange with water protons with T2 values in the range of 10-30 ms which are detected in qT2 experiments. There may be differences between these two proton pools in sensitivity to changes in the fraction of the bound proton pool related to lipid composition.

EC staining showed evidence of remyelination prior to changes in MWF. The proportion of EC positively stained tissue in the dorsal column increased significantly by 21 dpi. Although changes in MWF and MTR occurred later than histological changes, it may be possible to differentiate early remyelination from normal white matter using both techniques. If the MWF is near control values while the MTR remains lower could be indicative of repair, particularly if IE and long T2 water components are normal. One can hypothesize that MTR and qT2 together could help differentiate remyelination from inflammation and edema, which has been shown to mildly decrease MTR (Gareau et al., 2000, Stanisz et al., 2004). If edema was present then a slight decrease in MTR and an increase in the intracellular/extracellular T2 value or an increase in the long T2 component fraction may be observed. Further work is required to test these hypotheses.

CONCLUSION

We showed that it is possible to follow a time course of demyelination and repair in the lysolecithin model of MS in the spinal cord of a living mouse. These results are consistent with prior studies showing that although MWF and MTR are both sensitive to myelination, they may be specific to different physiological states (Vavasour et al., 1998, Gareau et al., 2000, Odrobina et al., 2005, Tozer et al., 2005). We hypothesize that early remyelination can be differentiated from normal white matter using both MTR and qT2 including characterization of the entire T2 distribution. Although changes in MWF and MTR occurred after histological changes were detected, quantitative MR provides an objective non-invasive outcome for the evaluation of disease progression and therapeutic intervention.

Acknowledgements

This work was funded by the MS Society of Canada, the Alberta Heritage Foundation for Medical Research, Informatics Circle of Research Excellence, the Canadian Institutes of Health Research, the National Institutes of Health (NIH RO1 EB002085), and the Canadian Foundation for Innovation.

References

Alberghina M, Viola M, Moschella F, Giuffrida AM. Myelination of regenerating sciatic nerve of the rat: lipid components and synthesis of myelin lipids. Neurochem Res 1983;8:133–150. [PubMed: 6190098]

Anastasiou A, Hall LD. Optimisation of T2 and M0 measurements of biexponential systems. Magn Reson Imaging 2004;22:67–80. [PubMed: 14972396]

Barkhof F, Bruck W, De Groot CJ, Bergers E, Hulshof S, Geurts J, Polman CH, van der Valk P. Remyelinated lesions in multiple sclerosis: magnetic resonance image appearance. Arch Neurol 2003;60:1073–1081. [PubMed: 12925362]

Beaulieu C, Fenrich FR, Allen PS. Multicomponent water proton transverse relaxation and T2-discriminated water diffusion in myelinated and nonmyelinated nerve. Magn Reson Imaging 1998;16:1201–1210. [PubMed: 9858277]

Biton IE, Duncan ID, Cohen Y. High b-value q-space diffusion MRI in myelin-deficient rat spinal cords. Magn Reson Imaging 2006;24:161–166. [PubMed: 16455404]

Bjarnason TA, Vavasour IM, Chia CL, MacKay AL. Characterization of the NMR behavior of white matter in bovine brain. Magn Reson Med 2005;54:1072–1081. [PubMed: 16200557]

Blezer EL, Bauer J, Brok HP, Nicolay K, t Hart BA. Quantitative MRI-pathology correlations of brain white matter lesions developing in a non-human primate model of multiple sclerosis. NMR Biomed 2007;20:90–103. [PubMed: 16948176]

Bonilla I, Snyder RE. Transverse relaxation in rat optic nerve. NMR Biomed 2007;20:113–120. [PubMed: 16998953]

Chen JT, Collins DL, Atkins HL, Freedman MS, Arnold DL. Magnetization transfer ratio evolution with demyelination and remyelination in multiple sclerosis lesions. Ann Neurol 2008;63:254–262. [PubMed: 18257039]

Cook LL, Foster PJ, Mitchell JR, Karlik SJ. In vivo 4.0-T magnetic resonance investigation of spinal cord inflammation, demyelination, and axonal damage in chronic-progressive experimental allergic encephalomyelitis. J Magn Reson Imaging 2004;20:563–571. [PubMed: 15390226]

Davies GR, Ramani A, Dalton CM, Tozer DJ, Wheeler-Kingshott CA, Barker GJ, Thompson AJ, Miller DH, Tofts PS. Preliminary magnetic resonance study of the macromolecular proton fraction in white matter: a potential marker of myelin? Mult Scler 2003;9:246–249. [PubMed: 12814170]

Deloire-Grassin MS, Brochet B, Quesson B, Delalande C, Dousset V, Canioni P, Petry KG. In vivo evaluation of remyelination in rat brain by magnetization transfer imaging. J Neurol Sci 2000;178:10–16. [PubMed: 11018243]

Does MD, Snyder RE. Multiexponential T2 relaxation in degenerating peripheral nerve. Magn Reson Med 1996;35:207–213. [PubMed: 8622585]

Dousset V, Brochet B, Vital A, Gross C, Benazzouz A, Boullerne A, Bidabe AM, Gin AM, Caille JM. Lysolecithin-induced demyelination in primates: preliminary in vivo study with MR and magnetization transfer. AJNR Am J Neuroradiol 1995;16:225–231. [PubMed: 7726066]

Gareau PJ, Rutt BK, Bowen CV, Karlik SJ, Mitchell JR. In vivo measurements of multi-component T2 relaxation behaviour in guinea pig brain. Magn Reson Imaging 1999;17:1319–1325. [PubMed: 10576717]

Gareau PJ, Rutt BK, Karlik SJ, Mitchell JR. Magnetization transfer and multicomponent T2 relaxation measurements with histopathologic correlation in an experimental model of MS. J Magn Reson Imaging 2000;11:586–595. [PubMed: 10862056]

Gent WL, Gregson NA, Gammack DB, Raper JH. The Lipid-Protein Unit In Myelin. Nature 1964;204:553–555. [PubMed: 14238160]

Graham SJ, Stanchev PL, Bronskill MJ. Criteria for analysis of multicomponent tissue T2 relaxation data. Magn Reson Med 1996;35:370–378. [PubMed: 8699949]

Hall SM. The effect of injections of lysophosphatidyl choline into white matter of the adult mouse spinal cord. J Cell Sci 1972;10:535–546. [PubMed: 5018033]

Harry GJ, Goodrum JF, Bouldin TW, Wagner-Recio M, Toews AD, Morell P. Tellurium-induced neuropathy: metabolic alterations associated with demyelination and remyelination in rat sciatic nerve. J Neurochem 1989;52:938–945. [PubMed: 2918316]

Henkelman RM, Stanisz GJ, Graham SJ. Magnetization transfer in MRI: a review. NMR Biomed 2001;14:57–64. [PubMed: 11320533]

Jeffery ND, Blakemore WF. Remyelination of mouse spinal cord axons demyelinated by local injection of lysolecithin. J Neurocytol 1995;24:775–781. [PubMed: 8586997]

Kiernan JA. Chromoxane cyanine R. II. Staining of animal tissues by the dye and its iron complexes. J Microsc 1984;134:25–39. [PubMed: 6201616]

Kiernan, JA. Histological and Histochemical Methods: theory and practice. Pergamon Press; Toronto: 1990.

Kozlowski P, Liu J, Yung AC, Tetzlaff W. High-resolution myelin water measurements in rat spinal cord. Magn Reson Med 2008;59:796–802. [PubMed: 18302247]

Kucharczyk W, Macdonald PM, Stanisz GJ, Henkelman RM. Relaxivity and magnetization transfer of white matter lipids at MR imaging: importance of cerebrosides and pH. Radiology 1994;192:521–529. [PubMed: 8029426]

Larsen PH, Wells JE, Stallcup WB, Opdenakker G, Yong VW. Matrix metalloproteinase-9 facilitates remyelination in part by processing the inhibitory NG2 proteoglycan. J Neurosci 2003;23:11127–11135. [PubMed: 14657171]

Laule C, Leung E, Lis DK, Traboulsee AL, Paty DW, MacKay AL, Moore GR. Myelin water imaging in multiple sclerosis: quantitative correlations with histopathology. Mult Scler 2006;12:747–753. [PubMed: 17263002]

Laule C, Vavasour IM, Kolind SH, Traboulsee AL, Moore GR, Li DK, Mackay AL. Long T2 water in multiple sclerosis: what else can we learn from multi-echo T2 relaxation? J Neurol 2007a;254:1579–1587. [PubMed: 17762945]

Laule C, Vavasour IM, Madler B, Kolind SH, Sirrs SM, Brief EE, Traboulsee AL, Moore GR, Li DK, MacKay AL. MR evidence of long T2 water in pathological white matter. J Magn Reson Imaging 2007b;26:1117–1121. [PubMed: 17896375]

Levesque I, Sled JG, Narayanan S, Santos AC, Brass SD, Francis SJ, Arnold DL, Pike GB. The role of edema and demyelination in chronic T1 black holes: a quantitative magnetization transfer study. J Magn Reson Imaging 2005;21:103–110. [PubMed: 15666408]

Lucchinetti C, Bruck W, Parisi J, Scheithauer B, Rodriguez M, Lassmann H. Heterogeneity of multiple sclerosis lesions: implications for the pathogenesis of demyelination. Ann Neurol 2000;47:707–717. [PubMed: 10852536]

MacKay A, Laule C, Vavasour I, Bjarnason T, Kolind S, Madler B. Insights into brain microstructure from the T2 distribution. Magn Reson Imaging 2006;24:515–525. [PubMed: 16677958]

Markovic-Plese S, McFarland HF. Immunopathogenesis of the multiple sclerosis lesion. Curr Neurol Neurosci Rep 2001;1:257–262. [PubMed: 11898527]

Merkler D, Boretius S, Stadelmann C, Ernsting T, Michaelis T, Frahm J, Bruck W. Multicontrast MRI of remyelination in the central nervous system. NMR Biomed 2005;18:395–403. [PubMed: 16086436]

Minty EP, Bjarnason TA, Laule C, MacKay AL. Myelin water measurement in spinal cord. Magnetic Resonance in Medicine. 2009in press

Mottershead JP, Schmierer K, Clemence M, Thornton JS, Scaravilli F, Barker GJ, Tofts PS, Newcombe J, Cuzner ML, Ordidge RJ, McDonald WI, Miller DH. High field MRI correlates of myelin content and axonal density in multiple sclerosis--a post-mortem study of the spinal cord. J Neurol 2003;250:1293–1301. [PubMed: 14648144]

Odrobina EE, Lam TY, Pun T, Midha R, Stanisz GJ. MR properties of excised neural tissue following experimentally induced demyelination. NMR Biomed 2005;18:277–284. [PubMed: 15948233]

Papanikolaou N, Maniatis V, Pappas J, Roussakis A, Efthimiadou R, Andreou J. Biexponential T2 relaxation time analysis of the brain: correlation with magnetization transfer ratio. Invest Radiol 2002;37:363–367. [PubMed: 12068156]

Papanikolaou N, Papadaki E, Karampekios S, Spilioti M, Maris T, Prassopoulos P, Gourtsoyiannis N. T2 relaxation time analysis in patients with multiple sclerosis: correlation with magnetization transfer ratio. Eur Radiol 2004;14:115–122. [PubMed: 14600774]

Pavelko KD, van Engelen BG, Rodriguez M. Acceleration in the rate of CNS remyelination in lysolecithin-induced demyelination. J Neurosci 1998;18:2498–2505. [PubMed: 9502810]

Pirko I, Johnson AJ. Neuroimaging of demyelination and remyelination models. Curr Top Microbiol Immunol 2008;318:241–266. [PubMed: 18219821]

Rademacher J, Engelbrecht V, Burgel U, Freund H, Zilles K. Measuring in vivo myelination of human white matter fiber tracts with magnetization transfer MR. Neuroimage 1999;9:393–406. [PubMed: 10191168]

Rasband, W. ImageJ. U S National Institutes of Health; Bethesda, Maryland, USA: 19972007.

Ropele S, Strasser-Fuchs S, Augustin M, Stollberger R, Enzinger C, Hartung HP, Fazekas F. A comparison of magnetization transfer ratio, magnetization transfer rate, and the native relaxation time of water protons related to relapsing-remitting multiple sclerosis. AJNR Am J Neuroradiol 2000;21:1885–1891. [PubMed: 11110542]

Schmierer K, Scaravilli F, Altmann DR, Barker GJ, Miller DH. Magnetization transfer ratio and myelin in postmortem multiple sclerosis brain. Ann Neurol 2004;56:407–415. [PubMed: 15349868]

Schmierer K, Tozer DJ, Scaravilli F, Altmann DR, Barker GJ, Tofts PS, Miller DH. Quantitative magnetization transfer imaging in postmortem multiple sclerosis brain. J Magn Reson Imaging 2007;26:41–51. [PubMed: 17659567]

Sled JG, Pike GB. Quantitative imaging of magnetization transfer exchange and relaxation properties in vivo using MRI. Magn Reson Med 2001;46:923–931. [PubMed: 11675644]

Stanisz GJ, Kecojevic A, Bronskill MJ, Henkelman RM. Characterizing white matter with magnetization transfer and T(2). Magn Reson Med 1999;42:1128–1136. [PubMed: 10571935]

Stanisz GJ, Webb S, Munro CA, Pun T, Midha R. MR properties of excised neural tissue following experimentally induced inflammation. Magn Reson Med 2004;51:473–479. [PubMed: 15004787]

Stewart WA, MacKay AL, Whittall KP, Moore GR, Paty DW. Spin-spin relaxation in experimental allergic encephalomyelitis. Analysis of CPMG data using a non-linear least squares method and linear inverse theory. Magn Reson Med 1993;29:767–775. [PubMed: 8350719]

Sun SW, Liang HF, Trinkaus K, Cross AH, Armstrong RC, Song SK. Noninvasive detection of cuprizone induced axonal damage and demyelination in the mouse corpus callosum. Magn Reson Med 2006;55:302–308. [PubMed: 16408263]

Tipperman R, Kasckow J, Herndon RM. The fine structure of macrophages in lysolecithin-induced demyelination: a freeze-fracture study. J Neuropathol Exp Neurol 1984;43:522–530. [PubMed: 6470749]

Tozer DJ, Davies GR, Altmann DR, Miller DH, Tofts PS. Correlation of apparent myelin measures obtained in multiple sclerosis patients and controls from magnetization transfer and multicompartmental T2 analysis. Magn Reson Med 2005;53:1415–1422. [PubMed: 15906291]

Vavasour IM, Whittall KP, Li DK, MacKay AL. Different magnetization transfer effects exhibited by the short and long T(2) components in human brain. Magn Reson Med 2000;44:860–866. [PubMed: 11108622]

Vavasour IM, Whittall KP, MacKay AL, Li DK, Vorobeychik G, Paty DW. A comparison between magnetization transfer ratios and myelin water percentages in normals and multiple sclerosis patients. Magn Reson Med 1998;40:763–768. [PubMed: 9797161]

Webb S, Munro CA, Midha R, Stanisz GJ. Is multicomponent T2 a good measure of myelin content in peripheral nerve? Magn Reson Med 2003;49:638–645. [PubMed: 12652534]

Whittall KP, MacKay AL, Graeb DA, Nugent RA, Li DK, Paty DW. In vivo measurement of T2 distributions and water contents in normal human brain. Magn Reson Med 1997;37:34–43. [PubMed: 8978630]

Wolff SD, Balaban RS. Magnetization transfer imaging: practical aspects and clinical applications. Radiology 1994;192:593–599. [PubMed: 8058919]

Wu Y, Alexander AL, Fleming JO, Duncan ID, Field AS. Myelin water fraction in human cervical spinal cord in vivo. J Comput Assist Tomogr 2006;30:304–306. [PubMed: 16628052]

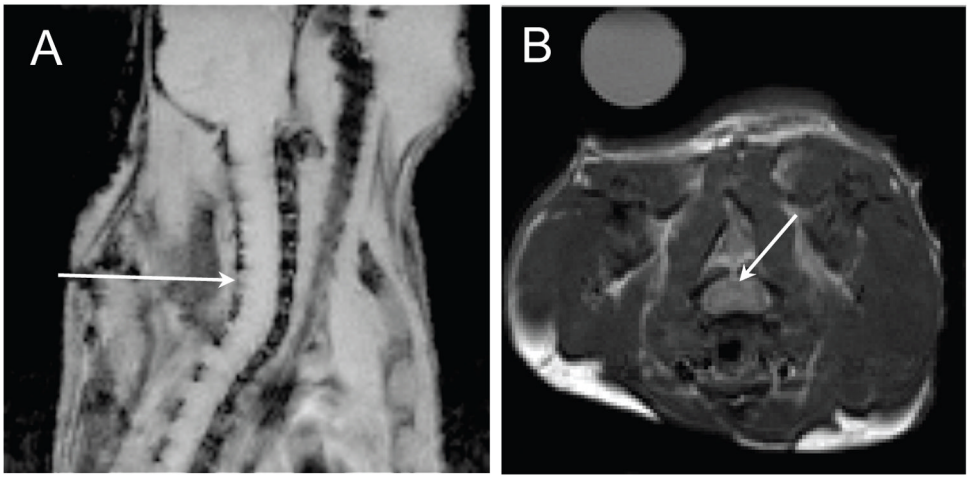

Figure 1.
Slice localization for quantitative MRI. The arrow in the FLASH sagittal scout image (A) indicates positioning of 0.75 mm transverse slices centered over the site of lysolecithin inject between C5 and C6 vertebrae. Intervertebral discs were used as landmarks for positioning. The corresponding T2-weighted transverse spin echo image (TR/TE=3s/15ms) with an arrow indicating the dorsal column is shown in (B). A tube containing distilled water was included as an external reference.

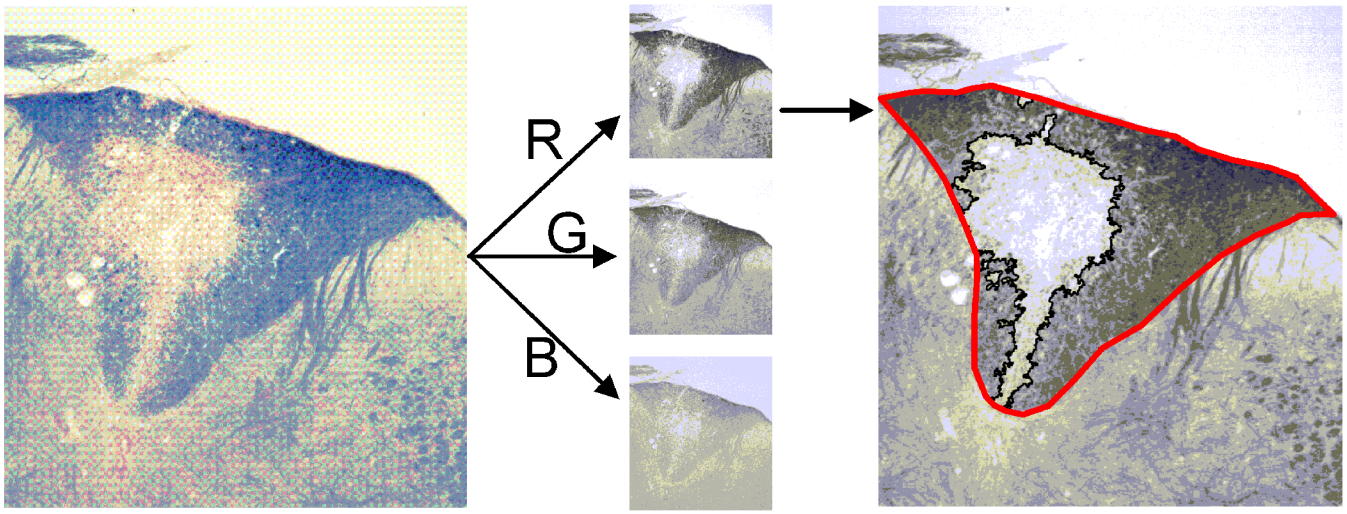

Figure 2. Histological quantification of lesion area using eriochrome cyanine staining for myelin

Color photomicrographs of EC-stained sections were converted to red, green, and blue channel grayscale images. The dorsal funiculus was manually outlined, intensity threshold applied, and the resulting lesion ROI automatically generated (outlined in black). The lesion area relative to the area of the dorsal funiculus was calculated. This analysis was performed using the red channel image as it had the best contrast between intact myelin and demyelinated lesions in the dorsal column.

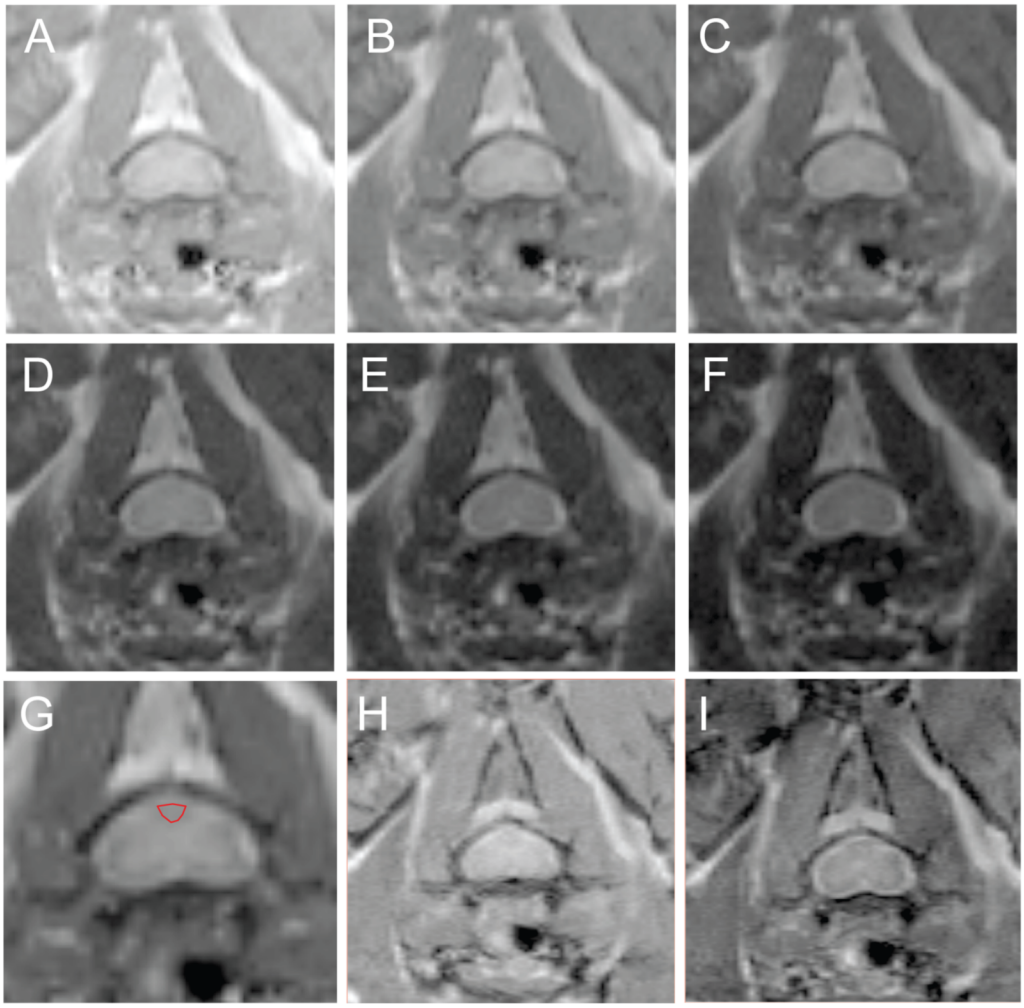

Figure 3. Axial spin echo images of the cervical spinal cord in one mouse

A sequence of images showing the signal decay over time is shown for TE=5, 15, 25, 35, 45, and 55 ms in A-F, respectively. Delineation between gray and white matter is most easily seen in the 25 ms echo image which has been enlarged in H and the dorsal column is outlined in red. Corresponding images (TR/TE= 4000/15 ms) without and with MT off resonance pulses applied (H) and (I) are shown.

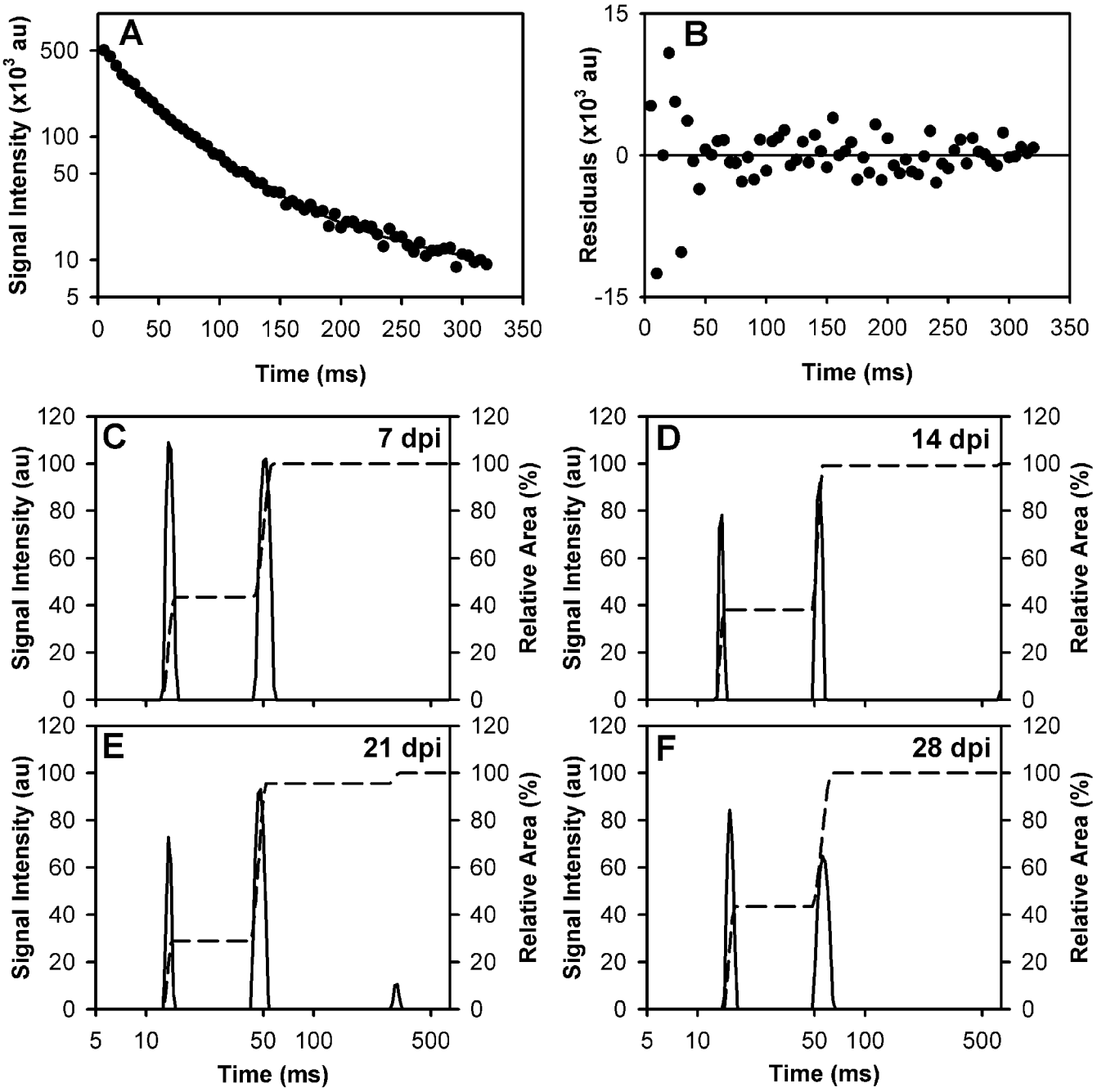

Figure 4. Example T2 signal decay curve and T2 distributions

The signal intensities from the multiecho images of a single mouse imaged at 21 days post injection (dpi) are plotted on a semi-log scale (A). The differences between the fit (solid line) and the data (B) are centered about zero. The corresponding regularized NNLS results for the same mouse on 7, 14, 21, and 28 days dpi are shown in C-F. The cumulative area of the T2 distributions is indicated by the dashed lines.

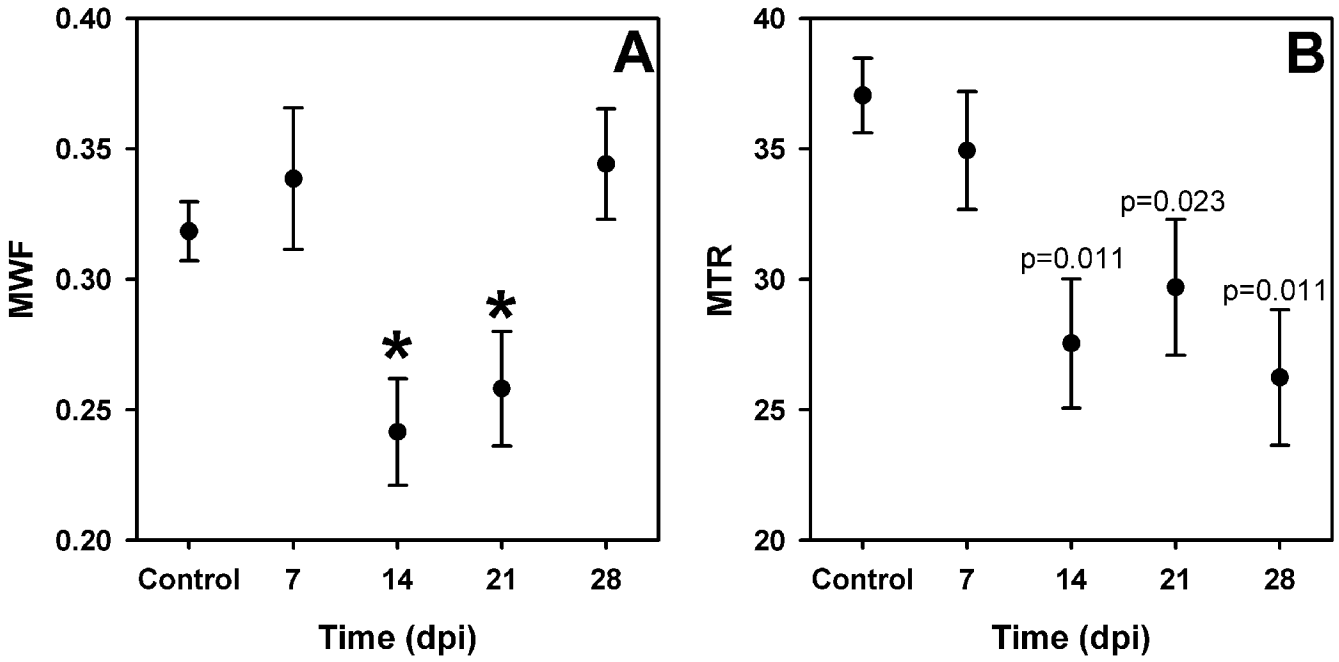

Figure 5. Time course changes in myelin water faction (MWF) and magnetization transfer ratio (MTR)

Mean values (±SEM) are shown for control (n=32) and lysolecithin-treated mice (n=10 and n=7 for MWF and MTR, respectively). The MWF for 14 and 21 days post injury (dpi) were significantly lower than 7, 28 dpi and control levels ($p<0.05$), indicated by the asterisks in (A). In contrast, the MTR values at 14, 21, and 28 dpi were significantly lower than control values only (B). MTR values significantly different from control levels are indicated by the p values above each point. The difference between MTR values for 7 dpi and 14 and 28 dpi approached significance, p=0.087 and 0.081, respectively.

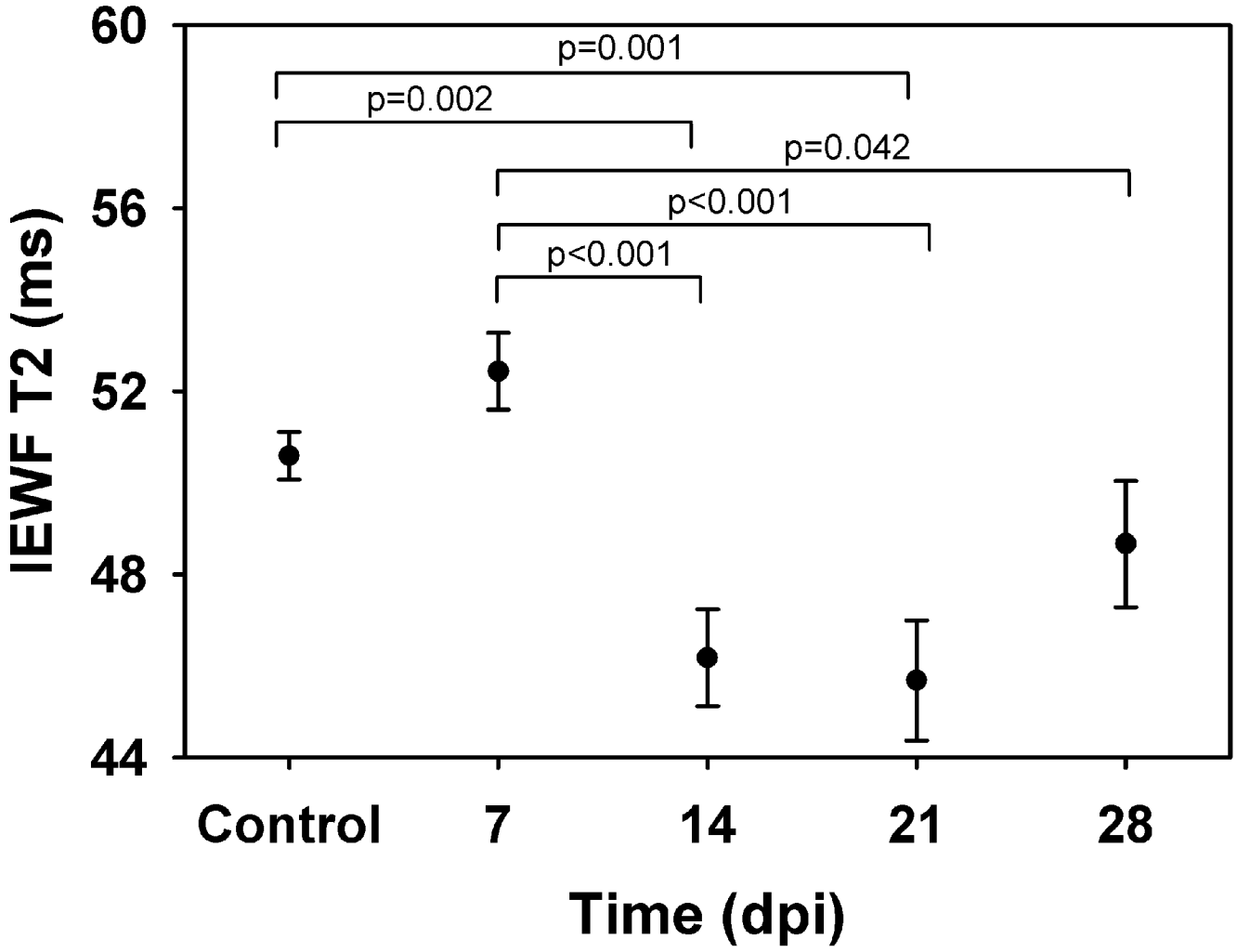

Figure 6.
Time course changes in intracellular/extracellular water fraction (IEWF) geometric mean T_2 values. Significantly different comparisons are indicated by the bracket with the p-value reported above the bracket. A significant decrease of 5ms was found between control and 14 and 21 dpi. The T2 values at 14, 21 and 28 dpi were significantly lower than 7 dpi.

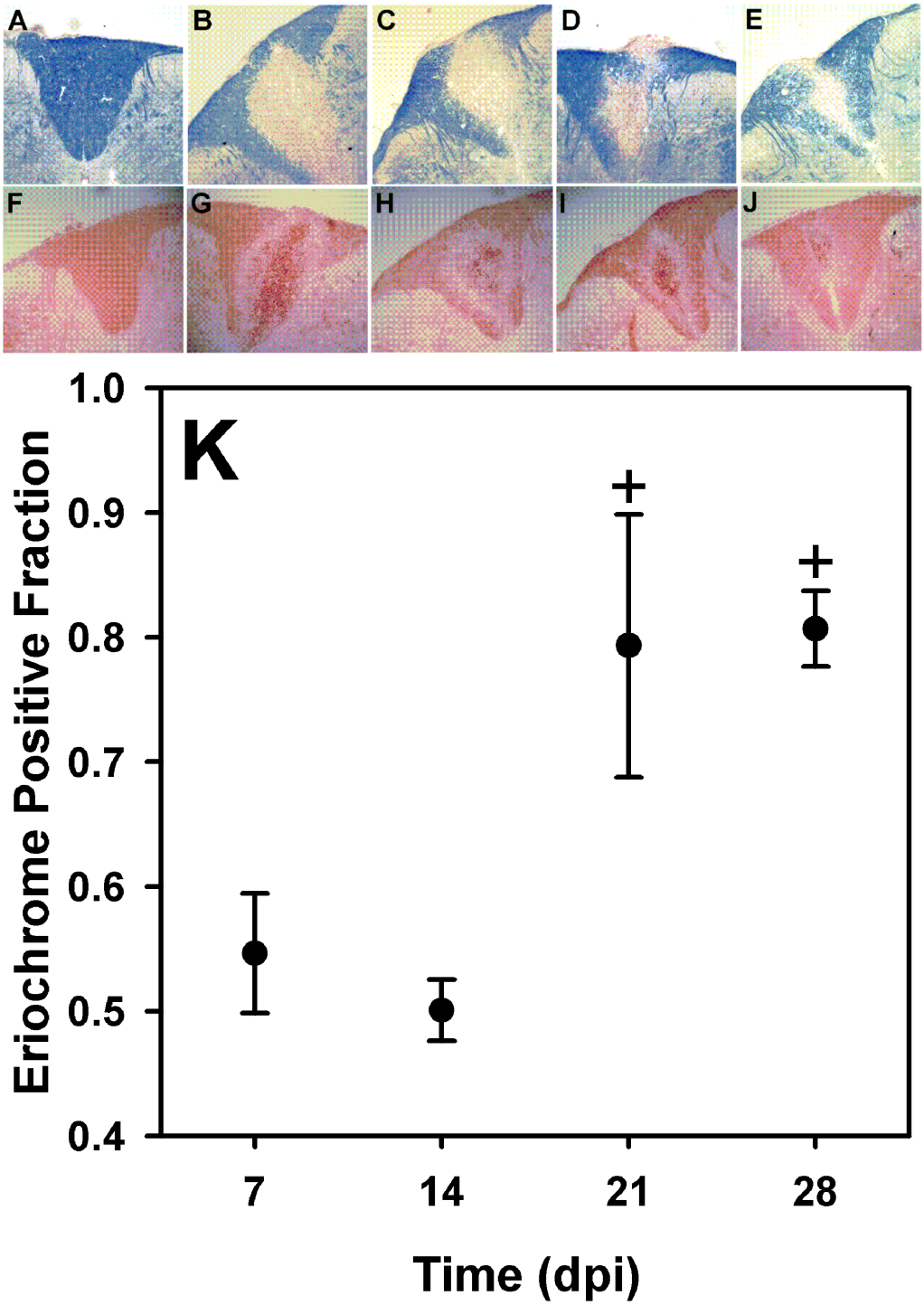

Figure 7. Micrographs of the dorsal column

Intact myelin appears blue in eriochrome cyanine-stained sections of the spinal cord. Spinal cord images from control, 7, 14, 21, and 28 dpi samples are shown in A-E, respectively. Oil red O-stained sections for control, 7, 14, 21, and 28 dpi samples are shown in F-J. Lipid appears red with darker droplets apparent in the lesion. Qualitatively, the number of dark droplets

decreased over time. The lesion size decreased to less than half of its size at 7dpi, shown in the graph of fractional area of EC staining in the dorsal column (mean ± SEM) (K).

Table 1

Summary of qT2 and magnetization transfer results (mean ± SEM).

	Fractional areas (%)			Geometric Mean T2			MTR
	Myelin (10-25 ms)	**IE (25-100 ms)**	**Long (>100 ms)**	**Myelin**	**IE**	**Long**	
Control	32 ± 1	67 ± 1	2 ± 1	12.7 ± 0.3	51 ± 1	490 ± 45	37 ± 1
7 dpi	34 ± 3	63 ± 2	3 ± 1	13.9 ± 0.8	53 ± 1	435 ± 67	35 ± 2
14 dpi	***24 ± 2***	***74 ± 2***	5 ± 1	12.4 ± 0.7	***46 ± 1***	392 ± 82	***28 ± 2***
21 dpi	***26 ± 2***	70 ± 3	5 ± 2	11.9 ± 0.6	***46 ± 1***	347 ± 63	***30 ± 3***
28 dpi	34 ± 2	64± 2	5 ± 2	13.3 ± 0.5	49 ± 1	341 ± 103	***26 ± 1***

Values in the lysolecithin-treated groups that are significantly different from the control values ($p<0.05$) are in bold italics.